Water Resources Research

RESEARCH ARTICLE
10.1029/2024WR038600

Increasing Large Precipitation Events and Low Available Water Holding Capacity Create the Conditions for Dry Land-Atmosphere Feedbacks in the Northeastern United States

Samuel Jurado[1,2] and **Jackie Matthes**[3]

[1]Department Earth and Atmospheric Sciences, Cornell University, Ithaca, NY, USA, [2]Now at School of the Environment, Yale University, New Haven, CT, USA, [3]Harvard Forest, Harvard University, Petersham, MA, USA

Key Points:

- Land-atmosphere coupling at Harvard Forest is principally controlled by the low amount of precipitation retained as soil moisture rather than evapotranspiration
- More extreme rainfall resulted in a greater percentage of water becoming unavailable to evapotranspiration due to low soil water holding capacity
- Drier soils are less capable of maintaining the necessary conditions for rain, which strengthens a amplifying dry soil moisture feedback loop

Supporting Information:

Supporting Information may be found in the online version of this article.

Correspondence to:

S. Jurado,
sam.jurado@yale.edu

Citation:

Jurado, S., & Matthes, J. (2025). Increasing large precipitation events and low available water holding capacity create the conditions for dry land-atmosphere feedbacks in the Northeastern United States. *Water Resources Research*, *61*, e2024WR038600. https://doi.org/10.1029/2024WR038600

Received 6 AUG 2024
Accepted 5 FEB 2025

Author Contributions:

Conceptualization: Samuel Jurado, Jackie Matthes
Data curation: Samuel Jurado
Formal analysis: Samuel Jurado
Funding acquisition: Jackie Matthes
Investigation: Samuel Jurado
Methodology: Samuel Jurado
Project administration: Jackie Matthes
Resources: Samuel Jurado
Software: Samuel Jurado
Supervision: Jackie Matthes
Validation: Samuel Jurado

Abstract As a warmer climate enables an increase in atmospheric humidity, extreme precipitation events have become more frequent in the Northeastern United States. Understanding the impact of evolving precipitation patterns is critical to understanding water cycling in temperate forests and moisture coupling between the atmosphere and land surface. Although the role of soil moisture in evapotranspiration has been extensively studied, few have analyzed the role of soil texture in determining ecosystem-atmosphere feedbacks. In this study, we utilized long term data associated with ecosystem water fluxes to deduce the strength of land-atmosphere coupling at Harvard Forest, Petersham, MA, USA. We found a 1.5% increase in heavy precipitation contribution per decade where high-intensity events compose upwards of 42% of total yearly precipitation in 2023. Intensifying precipitation trends were found in conjunction with a long-term soil drying at the Harvard Forest despite no significant increase in evapotranspiration over 32 years. This suggests that soil water holding capacity is a key mediating variable controlling the supply of water to ecosystems and the atmosphere. We found that these land surface changes directly impacted the lifted condensation level (LCL) height over Harvard Forest which was found to be increasing at a rate of 6.62 m per year while atmospheric boundary layer (ABL) heights have fallen at a modest rate of 1.76 m per year. This has amplified dry feedbacks between the land surface and the atmosphere such that 80% of observed summers ending in a water deficit also had an anomalously low soil water content in the spring.

Plain Language Summary Warm air holds more water. As air temperatures increase due to climate change, this warmer air evaporates more water from the soil and releases it in more intense rain events. Since the soils at Harvard Forest have a low water holding capacity, most of this rainfall quickly seeps deep into the ground and becomes unavailable for trees to take up through shallow roots or for the atmosphere to evaporate. Thus, despite more intense and total rainfall, the surface soils are becoming drier. These drier soils do not contribute as much water back to the atmosphere as is needed to maintain the conditions necessary for rain as often as wetter soils. As a result, drier soils do not create as much rain as wetter soils, and become even drier, creating an amplifying feedback loop. These results suggest that the amount of water available to the atmosphere within a soil is an important factor in creating the conditions necessary for strong interactions between the land and atmosphere in this region.

1. Introduction

Changes in the quantity and intensity of precipitation are critical climate change feedbacks that impact ecosystems and the people that depend on them. There is strong evidence for an amplifying water cycle at a global scale due to climate change, with increasing precipitation variability and extreme events (Douville et al., 2021). In the Northeastern United States, climate change and large-scale circulation patterns have caused more extreme precipitation events and higher total precipitation as a warmer climate enables an increase in atmospheric humidity (Huang et al., 2021; Olafsdottir et al., 2021). Within the Northeastern U.S., the relative change in extreme precipitation increased 50%–150% within the 1996–2018 time period when compared with a long-term 1920–1995 baseline period (Huang et al., 2021).

While precipitation and extreme rain events have increased in the Northeastern U.S., global studies have observed a seemingly counterintuitive decline in soil moisture in temperate forests. Global analyses at a 2.5-degree grid

Visualization: Samuel Jurado
Writing – original draft: Samuel Jurado
Writing – review & editing: Samuel Jurado, Jackie Matthes

scale with reanalysis and FLUXNET evapotranspiration data have attributed long-term soil drying trends within wet ecosystems to increased evaporative demand that creates higher rates of evapotranspiration (Qing et al., 2023). However, the timescales over which precipitation is delivered to ecosystems and retained as plant-available soil water, also known as the soil available water holding capacity (AWHC), is another factor that might influence overall soil moisture and land-atmosphere coupling.

Land-atmosphere coupling is defined as the degree to which the atmosphere responds to anomalies in land surface state (Koster et al., 2006). The positive soil moisture feedback loop is a form of land-atmosphere coupling that describes the tendency for initial surface moisture conditions to reinforce feedback mechanisms that amplify those initial conditions through energy flux partitioning as latent and sensible heat (Figure 1). Latent and sensible heat flux at the surface are well mixed by the turbulence generated by mechanical and buoyant eddies within the atmospheric boundary layer (ABL). Sensible and latent heat flux have significant impacts on the mean temperature and low-level moisture content of the ABL, respectively, which simultaneously influences the height of the lifted condensation level (LCL). Convective precipitation develops when an air parcel passes the LCL and has enough energy to overcome the negative buoyancy separating it from the level of free convection (LFC) (Siqueira et al., 2009). Thus, the timing of convective activation can be approximated by focusing on precipitation events that immediately follow the LCL intersecting the ABL. When the soils are wet, latent heat composes a greater fraction of the surface energy budget than sensible heat. This supplies the atmosphere with moisture while reducing its mean temperature by diminishing sensible heat flux. Both outcomes work to lower the LCL, which in turn increases the chances of convective precipitation formation and wetter soils. The reverse effect is achieved with drier soils, where latent heat is lower and sensible heat is higher, which raises the LCL. A previous study with long-term weather data from Northeastern U.S. airports found that cloud-ceiling height— and by extension the LCL—demonstrated a significant rising trend from 1973 to 1999 (Richardson et al., 2003).

The strength and nature of positive soil moisture feedback loops in humid midlatitude environments such as the Northeastern U.S. is still a subject of debate. Previous modeling studies within the GLACE experiment suggested that the Northeastern U.S. had negligible land-atmosphere coupling due to the region being dominated by an evaporation-limited wet (EL-W) regime (Koster et al., 2004). However, other studies have found that dry land-atmosphere feedback in the Northeastern U.S. may have significant impacts on the future of regional drought (Alessi et al., 2022). Most approaches to characterizing land-atmosphere coupling assume that since evapotranspiration in wet climates is not highly sensitive to variation in soil moisture, precipitation will not be sensitive to soil moisture either (Findell & Eltahir, 2003; Koster et al., 2004). The impact of soil texture and water holding capacity on the nonlinear interactions between precipitation intensity and soil moisture within the context of landscape scale land-atmosphere coupling remains understudied. Soil texture characterizes the available water holding capacity (AWHC) of a soil profile and determines water supply for latent heat flux to the atmosphere. The AWHC of a soil profile is the amount of water that is retained in the near-surface soil matrix after the deep drainage of precipitation and is determined by the soil texture and rock fraction (e.g., AWHC is lower, and drainage is faster in coarse soils with rocks). Water is transported from soils to the atmosphere by plant transpiration and soil evaporation when the vapor pressure deficit overcomes the soil matric potential. Since the relationship between soil water content and matric potential is generally considered to be logarithmic, soil moisture is far more available to the atmosphere at higher moisture values between field capacity and saturation. The amount of water transported to the atmosphere by transpiration and evaporation depends on two factors: the amount of time water stays near the surface before becoming lost to transport or deep percolation and the volume of water left in surface soils. In soils with low AWHC, ecosystems are more likely to develop an amplifying positive soil moisture feedback loop in which well drained soils retain a smaller fraction of the water supplied to them by heavy precipitation events. Thus, they have far less moisture available for evapotranspiration to the atmosphere than the total amount of precipitation received.

Northeastern U.S. landscapes have soils dominated by glacial till and fluvial soils low in clay and high in sand and silt as a result of periglacial erosion and deposition during the last glacial period. The alfisols, inceptisols, and spodosol soils composing the majority of the Northeastern U.S. are described as well drained (Ciolkosz et al., 1989, pp. 285–302). The AWHC of upland Northeastern U.S. soils is further reduced by rock fragments that compose upwards of 21% of the 50 cm profile by volume, constraining the AWHC of the top 50 cm to 4.6–7.2 cm, a relatively small capacity compared to the region's annual precipitation of 116.84 cm (Kern, J. S. 1995; Agel et al., 2015). Due to the increase in the amount of precipitation delivered in large events, the low AWHC of

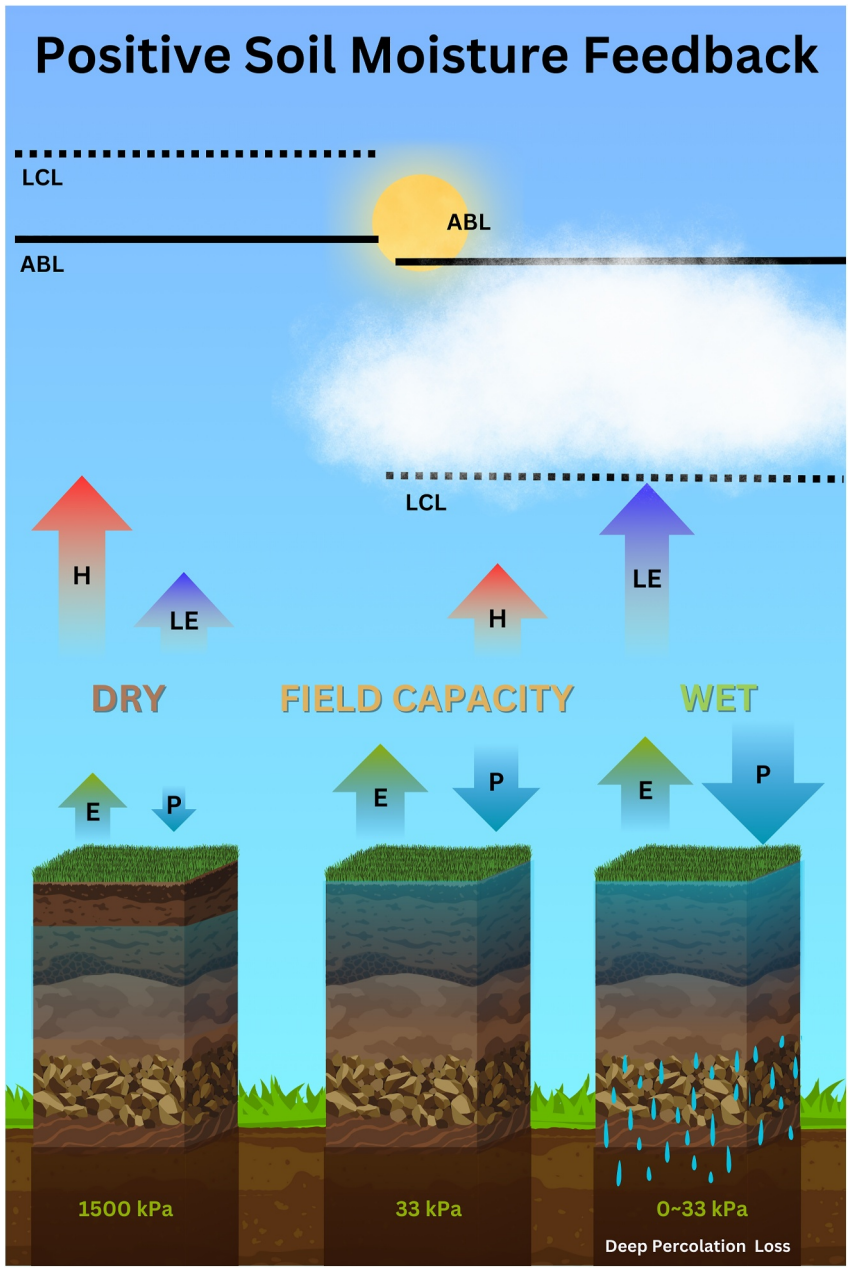

Figure 1. Schematic diagram of the mechanisms underlying a positive soil moisture feedback loop and evapotranspirative response to soil moisture conditions under differing precipitation rates. Red arrows represent sensible heat flux, (H) while blue arrows represent latent heat flux (LE). Solid lines are the atmospheric boundary layer (ABL) height while the dashed lined in the lifted condensation level (LCL). Green arrows represent evapotranspiration (E), while teal arrows represents precipitation (P). The size of the arrows correspond to the amount of water leaving or entering the system. The numbers represent the matric potential of each soil.

Northeastern U.S. soils might create conditions with lower overall soil moisture in uplands, as precipitation that exceeds the AWHC is lost to deep percolation and runoff.

Both droughts and extreme precipitation events are expected to increase with frequency as the climate warms (Hayhoe et al., 2007; Huang et al., 2021). The frequency and intensity of atmospheric aridity and soil drought is greatly increased by the presence of amplifying dry soil moisture feedbacks, which are projected to be further enhanced by global warming (Zhou et al., 2019). Under future climate regimes, regions such as the Northeastern U.S. and central Europe may become more favorable for land-atmosphere hydrological coupling due to the

amplification of atmospheric aridity under anonymously dry soil moisture conditions (Fischer et al., 2007). Increasingly dry feedback loops could potentially trigger cascading hydrological effects for the summer growing season, especially if they coincide with a spring onset when trees in seasonal climates are producing leaves.

In this study, we examine land-atmosphere coupling in a Northeastern U.S. temperate forest to characterize relationships among soil texture, soil moisture, and evapotranspiration in response to precipitation events during the growing season (May-September). We further investigate the connection among changing ecosystem water and energy fluxes and feedbacks to the atmospheric conditions that promote further precipitation. With long-term data collected from 1964 to 2023 at the Harvard Forest located in Petersham, MA we investigate three key research questions: (a) How have precipitation quantity and intensity, ecosystem soil moisture, and evapotranspiration changed on a multi-decadal timescale? (b) Does the intensity of precipitation events impact soil moisture, and in turn, rates of evapotranspiration? (c) Do changes in the local surface soil moisture state impact land-atmosphere coupling by influencing the atmospheric boundary layer (ABL) and lifted condensation level (LCL) heights? 4) Do soil moisture feedbacks allow spring conditions to influence summer drought vulnerability through land-atmosphere coupling?

2. Methods

2.1. Site Overview

The Harvard Forest is a temperate forest in north-central Massachusetts within the New England region of the United States (42.5°N, 72.2°W) where elevations range from 220 to 410 m above sea level. Soils at the Harvard Forest reflect the geological history of glaciation, with acidic, stony, glacial tills on top of metamorphic bedrock (Munger et al., 2020). The mean annual temperature during the 1991–2020 time period was 8.20°C (mean January temp was −4.98°C and mean July temperature was 17.9°C) (Boose & Gould, 2024). The mean annual precipitation for 1991–2020 was 1.175 m, distributed relatively evenly throughout the year (Boose & Gould, 2024). Forest composition at the Harvard Forest reflects recovery from past agricultural land use (Foster & Aber, 2004). The dominant tree species are red oak (*Quercus rubra*), red maple (*Acer rubrum*), eastern hemlock (*Tsuga canadensis*), and white pine (*Pinus strobus*), where *Q. rubra* has been the dominant species responsible for carbon dioxide at the site since carbon flux measurements began in 1991 (Urbanski et al., 2007; Wofsy et al., 1993).

2.2. Harvard Forest Meteorological and Evapotranspiration Data

Data for total daily precipitation have been recorded since 1964 at Harvard Forest (Boose & Gould, 2024). Data collection with a new meteorological station began at hourly temporal resolution in 2001, and at 15-min temporal resolution since 2015 (Boose, 2024). Long-term daily precipitation data were used to test for trends in the frequency of days with extreme precipitation and total annual precipitation. We defined heavy precipitation days as days where the daily precipitation exceeded the tenth percentile of all non-zero daily precipitation aggregated over the entire time period (1964–2023).

We used eddy covariance measurements from the Harvard Forest Environmental Measurement Systems (EMS) tower (Ameriflux site US-Ha1) to quantify rates of evapotranspiration from 1992 to 2023 (Munger & Wofsy, 2024). Evapotranspiration (ET) data at the EMS tower were collected at hourly temporal resolution. Evapotranspiration data were filtered by ustar (surface friction velocity) thresholds calculated for two periods within each year: the growing season (leaf-on) and non-growing season (leaf-off) using the variable ustar FLUXNET methodology (Pastorello et al., 2020). To define the growing season start and end dates within each year, we used a Bayesian land-surface phenology model to estimate the start-of-season and end-of-season using Landsat EVI2 data (30 m spatial resolution) with a nine-pixel grid centered at the tower location (Gao et al., 2021). We set measured values to NA for turbulent fluxes (e.g., evapotranspiration) where ustar was lower than the seasonally variable ustar threshold for each seasonal time period. We then filled gaps within hourly ET data through the standardized marginal distribution sampling (MDS) approach (Pastorello et al., 2020) and calculated daily and annual sums of ET.

We used gap-filled EMS tower ET data to test for significant long-term trends in evapotranspiration (1992–2023) with the Mann-Kendall test and calculated the slope of significant trends by estimating Sen's slope for the site time series (Hipel & McLeod, 1994; Sen, 1968). We used half-hourly ET observations (non-gap-filled) from the National Ecological Observatory Network (NEON) flux tower located at Harvard Forest to test the short-term

responses to rain events and soil moisture fluctuations (NEON, 2024a). Additionally, we utilized AERONET Level 2 quality spectrophotometer data from the NEON HARV tower, located 130 m from the EMS tower. This data, which was screened for cloud cover, pre- and post-field calibrated, and quality assured, was used to estimate the atmospheric water column (NEON, 2024b).

2.3. Soil Moisture and Watershed Runoff Data

We used a set of soil moisture datasets to assess potential long-term trends in volumetric soil water content at four locations within the Harvard Forest EMS tower footprint: (a) continuous volumetric water content (VWC) sensors buried 15 cm below the ground surface at the EMS flux tower (2007–2022) and (b) HEM flux tower (2008–2022); (c) continuous VWC sensors buried 10 cm below the ground surface within an oak-dominated long-term biomass plot in the EMS footprint (2010–2022), and (d) bi-weekly to monthly manual sensor VWC measurements (1993–2003) and continuous sensor VWC measurements (2008–2021) integrated across the top 15 cm of the soil within control plots (unheated) at the Prospect Hill Soil Warming Experiment at Harvard Forest (Frey & Melillo, 2024; Matthes et al., 2024; Munger & Hadley, 2024). VWC sensor measurements are sensitive to variations in soil texture, which changes at the plot-scale within Harvard Forest. To compare trends among VWC datasets, we calculated the site-specific soil moisture anomaly as the difference between each sensor VWC measurement and the mean across the entire VWC time series specific to that sensor and site. We tested for significant long-term trends in VWC within each site using the Mann-Kendall test and estimated the Sen's slope for the site time series (Hipel & McLeod, 1994; Sen, 1968).

We also used five soil moisture sensors collocated at the NEON HARV site to calculate the volumetric soil water content anomalies over the growing seasons (June–September) of 2017–2023 in response to specific rain events (NEON, 2024d). Each sensor was buried 6 cm beneath the surface. Soil moisture values were subtracted from the seasonal mean of each soil moisture sensor and averaged together to get one mean soil moisture anomaly for the site. The dataset was then smoothed utilizing a running median smoothing function with a median window of 21. Soil moisture anomaly difference was defined as the difference between the mean soil moisture anomaly 3 hr prior to a rain event and 12 hr afterward. We classified soil moisture into “wet” and “dry” days, defined as days in which the mean volumetric soil moisture anomaly was above zero (wet) or below zero (dry), for comparison to land-atmosphere coupling variables.

We used streamflow data from a gaged primary stream at the site to assess the relationship between precipitation events and watershed runoff from 2008 to 2023 (Boose & VanScoy, 2024). We used stream stage data from the growing season measured by pressure transducers at 15-min intervals that were converted into stream flow rate in units of L per second with stream rating curves calculated within the stream. We calculated daily streamflow as the sum of 15-min data within each day, assuming the measurement represented the streamflow rate during the full 15-min interval. We divided each daily streamflow sum by the watershed area (65 ha) to calculate the daily watershed runoff measured at the stream gage in mm. To pair watershed runoff data with precipitation events, we calculated the runoff difference between daily measured values and the mean values of runoff for the prior 7 days (i.e., the watershed runoff anomaly). We then compared the magnitude of the watershed runoff anomaly to the sum of the prior 7 days precipitation. We also coded the number of precipitation events in the prior 7-day window that exceeded the 95th percentile for daily rain during our precipitation time series (1964–2023). We used ANOVA to test whether the number of extreme events significantly increased the watershed runoff anomaly and the Tukey Honestly Significant Difference test to assess whether the pairwise number of events were significantly different from each other.

2.4. Soil Texture and Holding Capacity

We computed the available water holding capacity (AWHC) for the study site using pedon descriptions from the NEON Harvard Forest soil pit data (NEON, 2024c). Harvard Forest is part of three USDA NRCS soil survey areas: MA614 - Worcester County, MA, Northwestern Part (88%), MA011 – Franklin County, MA (9%), and MA017 – Middlesex County, MA (3%) (NEON, 2024c). From the 18 NEON soil plot sites, HARV_001 and HARV_005 were selected for AWHC calculation due to their proximity to NEON HARV tower's soil moisture sensors. Both belong to the Montuak-Canton association, feature 3%–35% slope, and are extremely stony with moderately well to well-drained till. These plots, along with others of the same soil series association, represent at least 14.3% of all Massachusetts soil survey areas and 28.21% of NEON HARV sample sites. Approximately 96%

of all NEON megapit sites at Harvard Forest were classified as moderately well to well-drained, and 82% were categorized as skeletal—characterized by a rock fragment content exceeding 35% within the first 50 cm. Water retention differences by texture were obtained from Finzi et al. (1960:354–363). AWHC was calculated for a profile assumed to be soil-only by multiplying layer thickness by its respective water retention difference and for a profile assuming that soil volume occupied by rock fragments held no water—an overestimation and underestimation, respectively (Robertson et al., 2021). For this study we averaged AWHC across both HARV_005 and HARV_001 profile sites for both pure soil and rocky profiles (Table S1 in Supporting Information S1).

Finally, we quantified the responses of the soil moisture and watershed runoff anomalies in relation to precipitation by estimating parameters for the logistic function:

$$S = \frac{K \cdot S_0}{S_0 + (K - S_0)\, e^{(-r \cdot P)}}$$

In which S_0 is initial soil moisture or watershed runoff, S is resulting soil moisture or watershed runoff, P is precipitation, r is intrinsic growth rate, and K is "carrying capacity" (i.e., AWHC or maximum watershed runoff) of the soil or stream in response to precipitation. Both r and K are parameters numerically derived utilizing base R's nls function.

2.5. Thornthwaite Water Balance

We used the Thornthwaite water balance to determine conditions when the Harvard Forest was in a net water balance deficit or surplus (Thornthwaite & Mather, 1955). The precipitation and potential evapotranspiration totals required for calculating the Thornthwaite water balance were calculated using the ClimClass package in R, following the methodology outlined by Eccel et al. (2016). Precipitation and temperature data from the Harvard Forest (1964–2023) were used to calculate potential evapotranspiration (Boose & Gould, 2024). We assumed that once the AWHC was exceeded, all precipitation was considered surplus and was either lost through deep percolation or runoff. Furthermore, it was assumed that once the AWHC was depleted all additional evapotranspiration contributed to a negative water deficit. However, AWHC values were constrained to remain non-negative. The study adhered to the USDA's definition of a water year, commencing in October, and accounted for the addition or subtraction of water from that point onward. We defined an anomalously dry spring as one where the available water content (AWC) in May was below the 1964–2023 mean for that month. Conversely, an anomalously wet spring was defined as having an AWC in May above the 1964–2023 mean for that month. The summer AWC proceeding these springs was calculated as the AWC budget at the end of the August of each year.

2.6. Atmospheric Boundary Layer (ABL) and Lifted Condensation Level (LCL) Heights

We used the NCEP North American Regional Reanalysis (NARR) data to point-sample an 8-hr resolution time series of the atmospheric boundary layer height at Harvard Forest throughout the growing season (JJAS) from 1973 to 2023 (Mesinger et al., 2006). The data extraction was performed at the geographical coordinates 42.60564°N, −72.11015°E, corresponding to the center of a 0.3-degree (~32 km) resolution grid cell that is the closest in Euclidean distance to the HARV site. The NARR dataset has strong correspondence between reanalysis measurements and land truth (Luo et al., 2007). Subsequently, the time series was interpolated into 30-min resolution to align temporally with the observations at the NEON HARV sensor data. The height of the lifted condensation level (LCL) was calculated using hourly temperature, barometric pressure, and relative humidity data from the EMS tower with the mathematical expression and the R code provided by Romps (2017). We performed a chi-square test of independence with Yate's continuity correction to determine whether there is a significant association between soil moisture conditions ("Wet" and "Dry") and the occurrence of convective activation (when the ABL exceeds the LCL). The same procedure was repeated to test whether convective activation events were associated with precipitation of at least a 1 mm daily total.

3. Results

3.1. Long-Term Trends in Precipitation, Soil Moisture, and Evapotranspiration

We found a significant increase in heavy precipitation events and total precipitation (1964–2023), a decline in soil moisture (1993–2023), and no significant change in forest-atmosphere evapotranspiration (1993–2023) at the

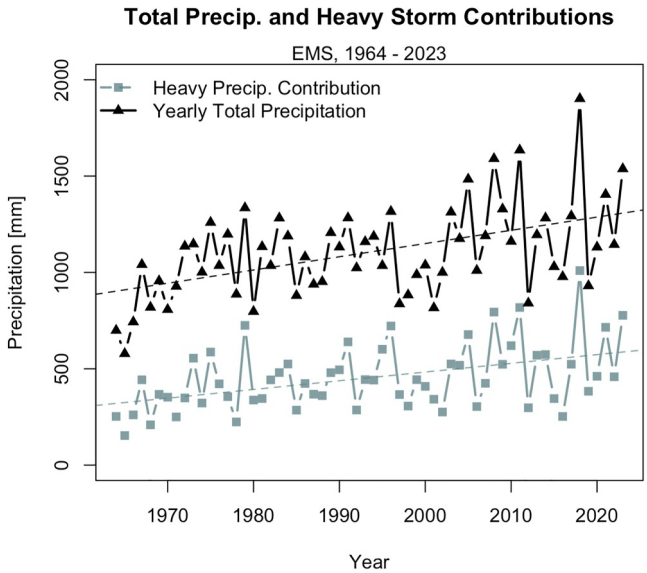

Figure 2. Long term Harvard Forest Climate data (1964–2023) showed a significant positive trend in precipitation (teal line, squares) contributed by heavy storms (top 10% over 40 years) during the 1946–2023 time period of 4.5 mm per year (Kendall's tau = 0.228, $p = 0.010$). The total amount of precipitation (black line, triangles) increased by 6.86 mm per year over the same time period (Kendall's tau = 0.315, $p = 0.0004$).

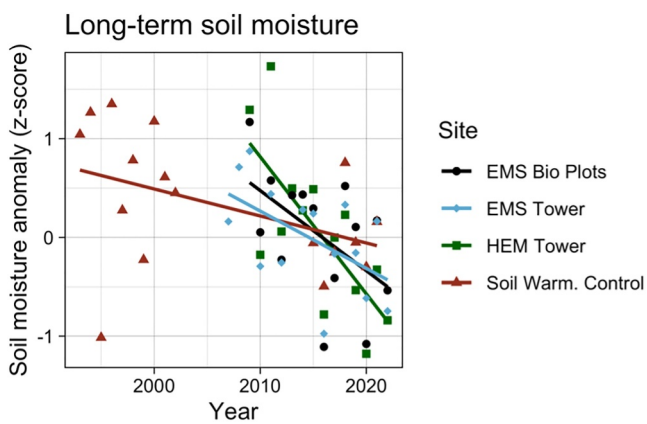

Figure 3. Seasonal means (May-Sept) of soil volumetric water content color coded by long term plot within Harvard Forest (Table S2 in Supporting Information S1). Solid lines indicate the best fit line to each respective plot trend. VWC anomaly is the departure from long term mean conditions within each plot. The Environmental Measurement Site (EMS) and the Hemlock (HEM) site are flux towers and their respective plots located within Harvard Forest.

Harvard Forest. The percent of annual precipitation contributed by heavy storms increased at a rate of 0.15% per year over the 1964–2023 time period (Kendall's tau = 0.23, $p = 0.010$) and the amount of precipitation delivered in heavy storms increased at a rate of 4.5 mm per year (Kendall's tau = 0.315, $p < 0.001$; Figure 2). Although the peak heavy storm contribution fraction occurred in 1995, the time period from 2005 to 2023 experienced six of the top 10 years with the highest heavy storm contribution ratio and seven of the top 10 years with the highest heavy storm precipitation totals since 1964. In 2010, 2011, 2018, 2021, and 2023, over 50% of yearly precipitation came from the top 10% of storms. The heavy storm contributions of the earliest recorded decade (1964–1974) averaged 35.4% of the yearly total precipitation while the latest decade (2013–2023) averaged 42.1%. Similarly, heavy storm precipitation totals increased from an average of 319 mm in 1964–1974 compared to 550 mm in 2013–2023. The highest heavy storm total occurred in 2018 with 1009 mm of precipitation, immediately preceded by 2011, 2008, and 2023 which produced 818 mm, 795 mm, and 777 mm of precipitation, respectively.

Despite the increase in large rain events, especially since 2005, average volumetric soil water content in May-September decreased between 1993 and 2022 at four independent long-term monitoring locations, with most rapid rates of drying in the past decade (Figure 3). Long-term soil drying at the Harvard Forest happened at a rate of −0.00341 to −0.0125 $m^3\ m^{-3}$ per year among the four long-term monitoring plots. Volumetric soil moisture declined between 1993 and 2021 at the Soil Warming Control Plots (Sen's Slope $S = -0.00341$, $p = 0.015$), between 2007 and 2022 at the EMS Tower ($S = -0.0104$, $p < 0.001$), and between 2009 and 2022 at the EMS Biometry Monitoring Plot ($S = -0.00352$, $p = 0.0375$) and Hemlock Tower ($S = -0.0125$, $p = 0.0062$; Full stats in Table S2 in Supporting Information S1) (Figure 4).

There was no significant trend in rates of June–September evapotranspiration during the 1992–2023 time period (Kendall's tau = −0.0161, $p = 0.91$) (Figure 4). The total amount of annual surplus water (annual precipitation minus annual evapotranspiration) increased at a rate of 7.105 mm per year throughout the 1991–2023 time period (Kendall's tau = 0.307, $p = 0.034$, Sen $S = 7.105$). There were 7 years with water deficits in which total evapotranspiration exceeded total precipitation with a range 11–130 mm of deficit. Five out of these seven water deficits occurred during the second half of the time period (since 2008), with multiple deficits near in time during 2016, 2019, and 2020.

The relationship between precipitation event size and soil moisture responses followed a logistic function that quickly saturated, where soil moisture increase and precipitation was significantly correlated only for precipitation events below 20 mm ($t = 9.056$, df = 127, $p < 0.001$). When precipitation exceeded 20 mm per event, soil moisture response values reached a peak value of 0.023 (logistic growth model; Std. Error = 0.0017, $t = 13.25$, $p < 0.001$). The differences in volumetric soil moisture gains based on initial wet or dry soil moisture conditions before precipitation were statistically significant, however the mean magnitude of these differences was less than 0.01 mm (difference of means = 0.0065 mm, $t(144.3) = 2.4269$, $p = 0.0165$). Thus, the limited soil moisture gains observed beyond 20 mm of precipitation were not due to variations in the initial wet or dry soil moisture condition at the surface.

The relationship for the sum of the prior weeks precipitation and watershed runoff anomalies followed a similar logistic pattern (Figure 5b). Daily watershed runoff only increased significantly for 7-day precipitation values that exceeded 50 mm rainfall ($t = 4.55$, df = 270, $p < 0.01$). Beyond a value of 50 mm for 7-day precipitation, the response of the watershed runoff anomaly

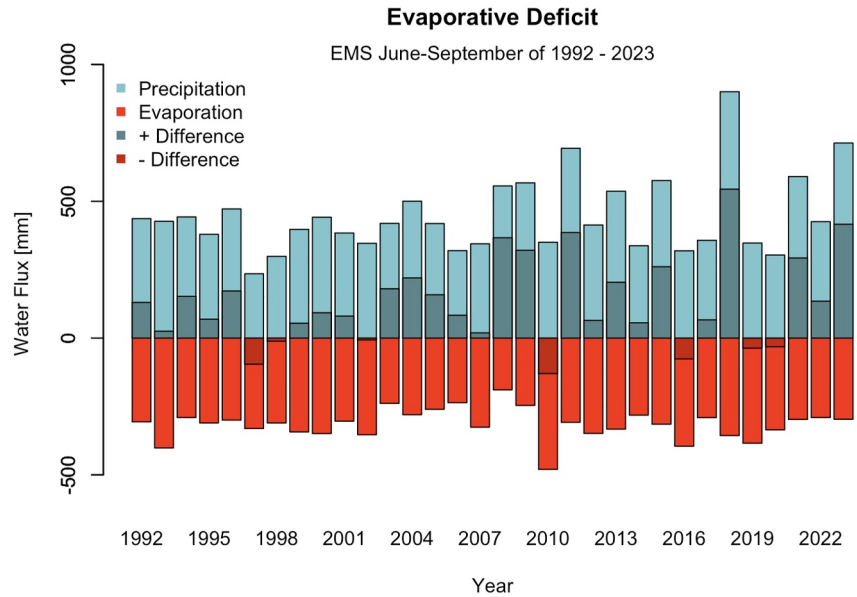

Figure 4. Yearly sums of growing season (June - September) precipitation totals (blue) and evaporation fluxes (red), and their positive (dark blue) or negative (dark red) differences. Data was sourced from the Environmental Measurement Site (EMS) at Harvard Forest from 1992 to 2023.

followed a logistic function that reached a peak value of 6.74 mm watershed runoff in response to an event size at 176 mm of weekly rainfall (logistic growth model; Std. Error = 1.76, $t = 4.85$, $p < 0.001$). The number of extreme precipitation events within the 7-day window (where daily precip exceeded the 1964–2023 95th percentile) had very small, but statistically significant, effects on the watershed runoff anomaly (ANOVA, $F(41,865) = 39.77$, $p < 0.001$). Having at least one extreme event within the prior week was related to a 0.39 mm higher watershed runoff than having no extreme events (Tukey HSD, $p = 0.00284$), two events increased runoff by 1.21 mm in comparison to one event (Tukey HSD, $p < 0.001$), three events increased runoff by 3.26 mm in comparison to two events (Tukey HSD, $p < 0.001$), and there was no significant difference between four and three extreme events within the week (Tukey HSD, $p = 0.956$).

3.2. Land-Atmosphere Coupling With Soil Moisture Conditions

Although the local long-term trend of soil moisture decreased while evapotranspiration did not change, the contribution of local evapotranspiration to the total atmospheric column water on clear-sky days increased with soil moisture when atmospheric vapor pressure deficit was high (Figure 6). The amount of water vapor in the atmospheric column under high vapor pressure deficits and clear-sky conditions (top 25% of VPD values) increased by 1.71% per cm of soil moisture anomaly (Kendall's tau = 0.301, $p = 0.0021$). There was no significant increase in local evapotranspirative contributions to the clear-sky atmospheric column with soil moisture anomaly under low vapor pressure deficit conditions (Kendall's tau = 0.0454, $p = 0.66$). Local evapotranspiration contributed 17.8% of water vapor to the clear-sky atmospheric column in average VPD conditions and upwards of 24.3% in high VPD conditions. In low VPD conditions, the local land surface contributed 10.9% of total column atmospheric water vapor in clear-sky conditions.

The soil moisture status at the land surface was strongly associated with the diurnal pattern of the lifted condensation level (LCL) height. Specifically, the mean LCL height during dry conditions was significantly higher than during wet conditions, indicating a positive feedback loop (difference of means = 158 m, $t(23,803) = 24.703$, $p < 0.001$; Figure 7).

The soil moisture status at the land surface was strongly associated with the diurnal pattern of the lifted condensation level (LCL) height; specifically, the mean LCL height during dry conditions was significantly higher than the mean LCL height in wet conditions, indicating the presence of a positive feedback loop (difference of means = 158 m, $t(23,803) = 24.703$, $p = <0.001$; Figure 7). There was also a small, but statistically significant,

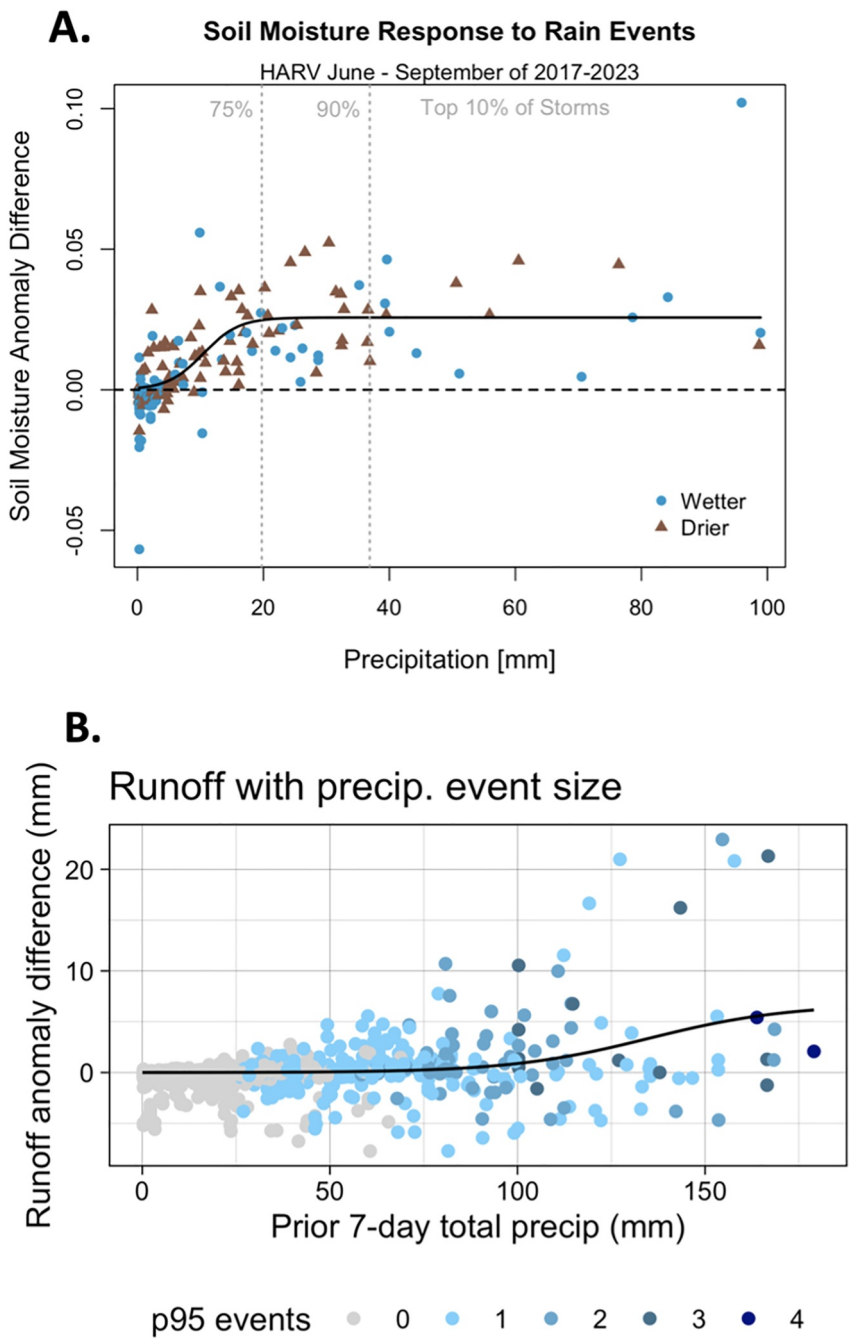

Figure 5. (a) Soil moisture anomaly and precipitation data was sourced from the NEON HARV tower at Harvard Forest throughout the growing season (June - September) from 2017 to 2023. The difference between mean soil moistures the 3 hr before and 12 hr after a rain event are plotted against the summed precipitation of that event. All rain events have a cumulative total of at least 0.3 mm. The black line is a nonlinear regression model. Brown points indicate that the mean soil moisture immediately prior to a rain event was drier than average, while blue points indicate the soils were wetter than average. The gray vertical lines indicate precipitation percentiles. (b) Daily watershed runoff data was sourced from a gaged primary stream at the NEON HARV site. The difference between daily measured values and mean runoff values for the prior 7 days were plotted against the sum of precipitation events of the prior 7-day precipitation. Point color corresponds to the number of 95th percentile rain events of the time series (1964–2023) that occurred during the 7-day window.

difference in ABL heights under dry and wet conditions (difference of means = 21.83 m, $t(24{,}116) = 3.5531$, $p = <0.001$). The mean relative humidity was significantly lower on days with drier soil conditions than on days with wetter conditions (difference of means = 5.69%, $t(24{,}040) = -25.047$, $p = <0.001$). There are small but

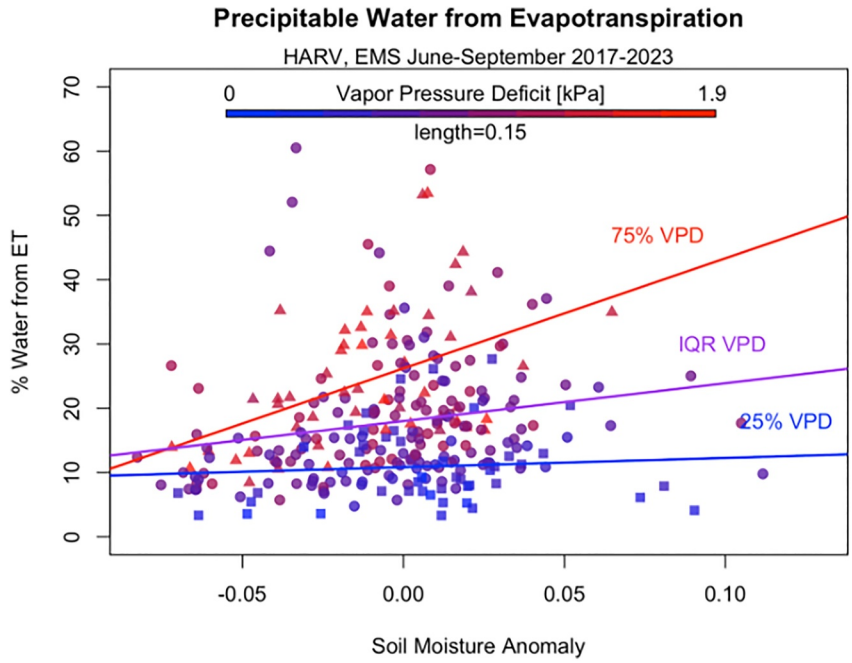

Figure 6. Soil moisture anomaly is plotted against the percent of water in the daily water column that is attributable to local evapotranspiration. The color of the points corresponds to the vapor pressure deficit (VPD) in which they were observed. The squares represent wetter (bottom 25th percentile VPD) atmospheric conditions, while the triangles and line represent drier conditions (top 25th percentile VPD). The circles represent the data points that fall within the interquartile range (IQR). Each line is a linear regression of the respective points that fall within the specified VPD quartile.

statistically significant differences in the expected direction of H, LE, and temperature (difference of 2.36 W, −0.063 mol/m^2/s (−2.56 W), and 0.68 C). We found that convective activation had a 81.39% chance of occurring over wetter soils, which was significantly greater than the 68.64% chance of occurring over drier soils (X-squared = 11.023, $p = 0.0009$). Additionally, the chance that precipitation would form after convective activation was greater over wetter soils (50%) than drier soils (36.23%) (X-squared = 9.9604, df = 1, $p = 0.0016$). Rain events that occurred during dry soil moisture conditions produced significantly smaller volumes of precipitation than in wet soil moisture conditions (difference of means = 5.7 mm, $t(171) = -2.43$, $p = 0.016$).

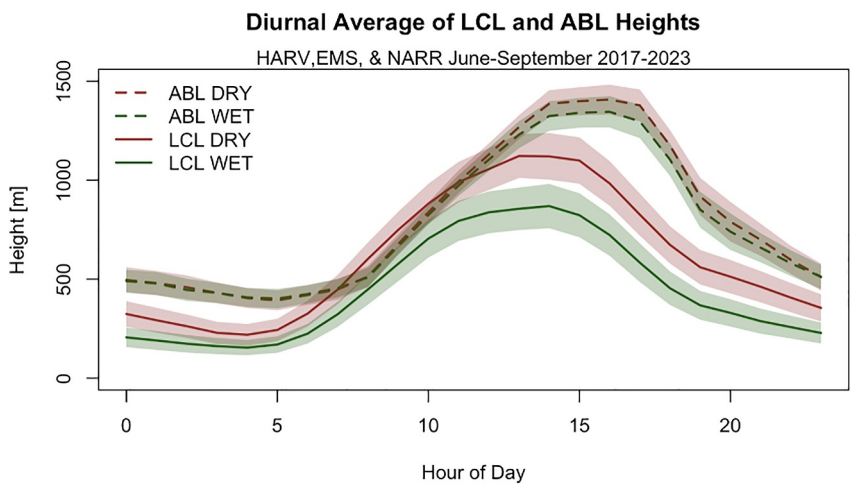

Figure 7. This plot portrays the diurnal average of atmospheric boundary layer (ABL) (dashed) and lifted condensation level (LCL) (solid) heights of Harvard Forest for the months of June through September from 2017 to 2023. The brown lines represent dry conditions while the green lines represent wet conditions (less than or greater than the mean soil moisture anomaly, respectively). The shaded areas correspond to the standard error of the diurnal average.

The LCL height responded dynamically to surface soil moisture conditions, with a more muted response in the ABL height and the net radiation flux at the surface. When soil moisture is below field capacity (a soil moisture anomaly of approximately 0), the average LCL and ABL heights are 547 m ± 25.8 and 779 m ± 29.3 m, respectively. After the soils reach field capacity but before stabilization at 0.075 m^3 m^{-3}, water becomes more available to the atmosphere, increasing relative humidity and causing the LCL height to fall at a rate of 56.9 m cm^{-1} soil water (Kendall's tau = −0.602, $p < 0.001$). After surpassing a soil moisture anomaly of 0.05 m^3 m^{-3}, the system becomes energy limited and LCL height stabilizes at 205 m ± 22.5 m. Compared to the LCL rate, the ABL height falls at a slower rate of 27.1 m cm^{-1} soil water (Kendall's tau = −0.275, $p = 0.0066385$) after surpassing field capacity. Below field capacity, the maximum net radiation achieved per soil moisture bin averaged 708 W m^{-2} while the wet regime averaged 389 W m^{-2}, indicating the increased presence of clouds over wetter soils.

Over the 1992–2023 time period there was a large and significant increase in average growing season LCL height, and a small decline in ABL height (Figure). The monthly mean LCL heights significantly increased at a rate of 6.62 m per year throughout the 1992–2023 time period (Kendall's tau = 0.431, $p < 0.001$). Average monthly ABL heights decreased at a more modest rate of 1.76 m per year over the 1979–2023 time period (Kendall's tau = −0.37, $p < 0.001$). LCL height is significantly negatively correlated to net summer precipitation influx (Pearson tau = −2.564, $p = 0.0158$, df = 29). For years above the 1992–2023 seasonal mean LCL height of 590 m ($n = 11$), 72.7% of all observed summers ended in anomalously dry conditions (lower precipitation minus evaporation values than mean), and 36.3% ended in a water deficit (precipitation minus evaporation less than zero). Below average LCL heights of 590 m ($n = 20$), only 40% of summers ended in anonymously dry conditions with 15% of years in a water deficit. Mean summer distance between the ABL and LCL is rapidly decreasing, and could intersect as early as 2044 if we extrapolate the time series relationships in this data.

Soil moisture conditions in spring may relate to the water deficit or surplus status at the end of the growing season. Although there was not a significant difference in summer available water content (AWC) between the dry and wet spring conditions, the results strongly suggest that drier springs are followed by drier growing seasons (difference of means = 25.2 mm, $t(56) = 1.9335$, $p = 0.0582$). Of the observed summers, 80% that ended in a water deficit also had an anomalously low AWC in the spring. Dry springs ($n = 34$) have a 35.3% chance of summer deficit, while wet springs ($n = 26$) have a 15.4% chance of ending in a water deficit. There was no significant difference in the magnitude of summer water deficits between dry and wet springs, which may be attributed to the limited occurrences of a wet spring followed by a deficit summer ($n = 3$) compared to a dry spring followed by a deficit summer ($n = 12$) (difference of means: 21.9 mm, $t(3.43) = 1.37$, $p = 0.254$). Similarly, no significant difference was observed in the magnitude of summer water surplus between dry and wet springs. This suggests that positive wet soil moisture feedbacks developing during the growing season may offset the effects of a drier spring (difference of means: 20.36 mm, $t(0.49) = 0.49$, $p = 0.637$).

4. Discussion

4.1. Water Balance Shifts

Both the amount of precipitation contributed by heavy storms and the fraction of total yearly precipitation attributable to heavy storms has increased significantly over the past 40 years at the Harvard Forest. Thus, an increasing amount of moisture supplied to Harvard Forest originates from short and intense storms as opposed to higher frequency storms of lower magnitude. This trend is particularly noticeable after 2010, during which the top four highest heavy precipitation totals on record occurred, coinciding with 5 years when heavy storm precipitation constituted the majority of the growing season precipitation (Figure 2). Our results of a 1.5% increase in heavy precipitation contribution per decade is comparable to the increase of 1.3%–1.6% in wet day precipitation per decade found in a recent global analysis (Feldman et al., 2024).

Despite the net increase in precipitation, Harvard Forest's soils have experienced a significant drying trend over the past 10–20 years. Although the global trend of drying soils coincident with excess precipitation has previously been attributed to increased evaporative demand, our results show that the growing season evapotranspiration flux at Harvard Forest has not significantly increased over the past 30 years. Since total precipitation and heavy precipitation have increased during this time period while soils have dried and evapotranspiration rates are unchanged, the excess moisture delivered to the ecosystem must have exited via percolation and runoff.

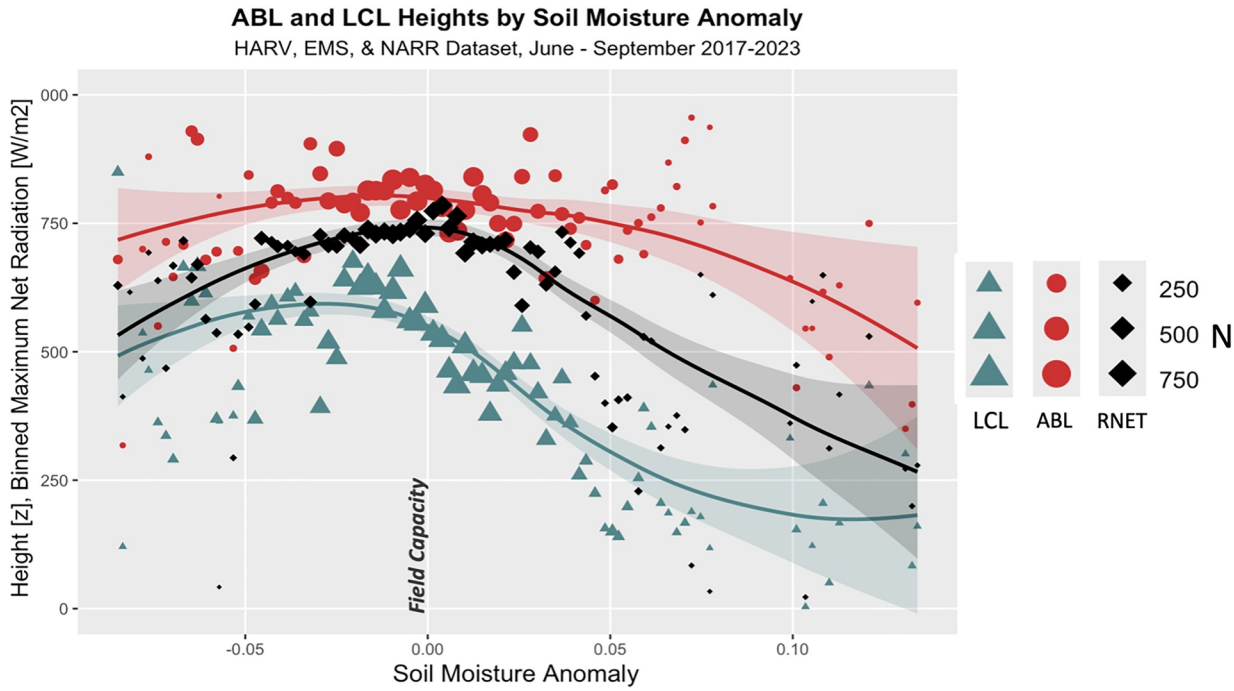

Figure 8. Soil moisture, net radiation (diamond), LCL (triangle), and ABL (circle) height data were sourced or calculated from the NEON HARV tower, EMS tower, and NARR dataset during the growing season (June–September) from 2017 to 2023. Each point represents the average LCL/ABL height within one of 75 soil moisture bins, with net radiation points showing the maximum value per bin. Point size reflects the number of observations, with the smallest bins containing at least 10 data points. Lines are weighted loess curves, with shaded areas indicating 95% confidence intervals.

4.2. Soil Water Holding Capacity Controlled System

Harvard Forest's soils have a limited water holding capacity due to their alluvial sandy composition and high rock fragmentation volume. Once the soils surpass field capacity, excess moisture is rapidly lost to deep percolation. Thus, infrequent, high-intensity events have greater runoff losses than frequent, low-intensity events. It follows that since these high-intensity events now compose upwards of 42% of total yearly precipitation (Figure 2), a greater portion of precipitation is lost to deep percolation and runoff. This is evidenced by the logistic growth of soil moisture and the modest gains in runoff during increasingly intense rain events (Figures 5a and 5b). While moderate increases in runoff are observed with both rising total rainfall and a higher frequency of heavy precipitation events, it is important to note that these small gains under extreme conditions likely reflect increased deep percolation losses. The rapid deep drainage associated with heavy rainfall events limits how much water remains in the top few centimeters of soil and available to the atmosphere. Unless promptly refilled, both low and high intensity rain events can cause soils to rapidly lose their moisture to evaporative demand. Smaller rainfall pulses infiltrate soil profiles less due to an increased soil evaporation and interception proportion relative to rainfall, thus reintroducing the majority of supplied moisture back into the atmosphere (Feldman et al., 2024). Soil moisture at field capacity in well-drained soils is fleeting during the growing season and is reliant upon moderate periodic precipitation refills as opposed to intense and infrequent rain pulses.

4.3. Land Atmosphere Coupling and Convectively Active Conditions

At low soil moisture levels, the land-atmosphere system is characterized by a decoupled dry regime in which moderate gains in soil moisture are temporary and insufficient to act as a significant source of local evapotranspiration. Once soil moisture levels surpass field capacity, water becomes more readily available for the atmospheric uptake and the system enters a transitional regime, in which soil moisture is directly coupled to LCL height and convective activation (Figure 8). As a result of increasing relative humidity at the surface, the LCL height decreases rapidly. We found an increase in cloud base height (LCL) of 6.62 m per year over Harvard Forest that is slightly larger than the results from a previous study in the Northeastern U.S. study that found an increasing cloud ceiling height of 4.14 ± 1.03 m per year from 1973 to 1999 (Richardson et al., 2003).

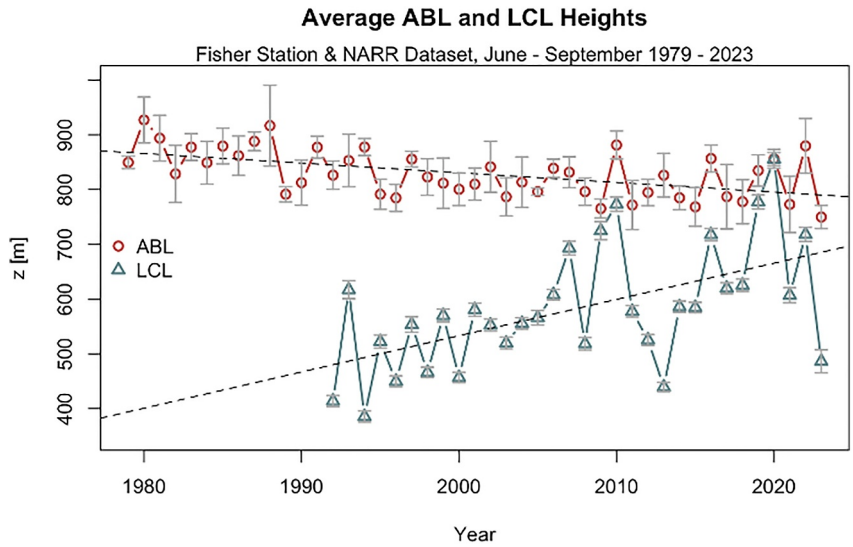

Figure 9. Average of atmospheric boundary layer (ABL) and lifted condensation level (LCL) height [m] for the months of June - September. LCL observations were calculated from EMS tower data at Harvard forest from 1992 to 2023, while ABL data from 1979 to 2023 was sourced from the NARR dataset. Error bars represent standard error, while dashed lines indicate the linear regression of the time series.

At higher soil moisture levels, the system enters an energy-limited regime, characterized by the lack of correlation among soil moisture, evapotranspiration, and LCL height (Figures 6 and 8). Evapotranspiration at high soil moisture levels is hindered by both a reduction in net radiation due to cloud development and a reduced moisture gradient between the soils and the air. Thus, atmospheric coupling is important for incoming photosynthetically active radiation (PAR) in North America (Green et al., 2017), which can have important impacts on photosynthesis (Humphrey et al., 2021). The ABL is highest under dry soil conditions, and undergoes a moderate decrease once the system enters an energy limited regime (Figure 8). This is likely due to both the reduction in sensible heat flux accompanying the decrease in net radiation and air being pumped out of the boundary layer via strong thermal plumes penetrating the ABL inversion through convective clouds activated by LCL crossover (Lee, 2018).

At lower soil moisture, the resulting reduction in surface humidity increases the height of the LCL. The decreasing seasonal mean distance between the LCL and ABL heights lowers the likelihood of crossover events and the subsequent convective activation required for precipitation formation, aligning with the findings of Alessi et al. (2022). In post-rainfall dry spells, soil moisture decreases, VPD increases, and downwelling surface radiation increases as clouds dissipate. This process encourages drying throughout the soil-plant-atmosphere continuum and perpetuates longer dry spells (Feldman et al., 2024). In addition to the significant increase in LCL height, the interannual variability of LCL heights has also increased. The maxima and minima of the increasingly variable fluctuations in LCL height roughly correspond to years of drought and flood within the Northeastern U.S. (Figure 9).

Except for the top quartile of the wettest atmospheric conditions, a higher soil moisture anomaly also increases local evapotranspirative contribution to the atmospheric column (Figure 6). For lower soil moisture values, a greater percentage of atmospheric moisture must be sourced from the free atmosphere as opposed to evapotranspiration from the surface in order to trigger convective events. As a result, rainfall over dry soils depends more on advected moisture than rainfall over wetter soils. Therefore, more rain would occur over wetter soils under comparable advective conditions since the moisture supplied by the atmosphere may not be enough to trigger a convective event over drier soils. The coupling between soil moisture and VPD is also highly dependent on net radiation (Figure 8), which is consistent with a prior study that found at low moisture levels, net radiation is enhanced by the dissipation of clouds (Gu et al., 2006). High net radiation enables an increase in evapotranspirative transfer as soil moisture increases so long as VPD is also high, while low net radiation coupled with low VPD may cause the Bowen ratio to change very little with soil moisture even when the soil is dry. When the

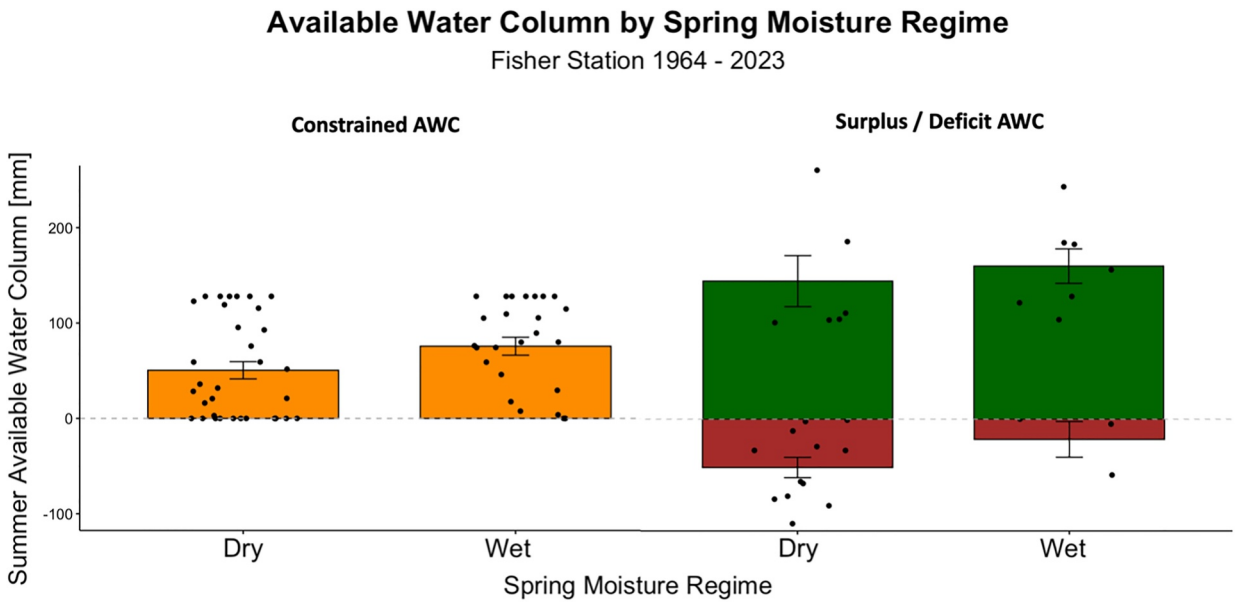

Figure 10. The orange bar graph represents the available water column at the end of summer (September 1st) following either a wet (above average AWC) or dry (below average AWC) spring (May). The overlaying black dots represent the datapoints that compose a one-dimensional scatterplot of each moisture regime. Here, the water column is assumed to hold a maximum of 128 mm of water, and a minimum of 0. The brown and green bar graphs portray the AWC deficit and surplus at the end of summers following wet or dry springs, respectively. The surplus and deficit bars represent the potential water loss or gain due to precipitation or evaporation if the water columns were not constrained between 0 and 128 mm. The error bars in all graphs capture the standard error of the portrayed dataset.

soil is wet, the increase in VPD dampens the increase of the Bowen ratio with net radiation by increasing latent heat flux and by extension the atmospheric water column (Gu et al., 2006).

4.4. Effects on Precipitation Events and Seasonal Recharge

Both the chances of convective activation, that is, crossover events, and the amount of precipitation from summer storms are enhanced with higher soil moisture and are suppressed in dry soil conditions. This mechanism creates the potential for positive soil moisture feedback loops to influence the local climate on a seasonal scale. Anomalously wet or dry springs may trigger a positive soil moisture feedback loop that may exacerbate extreme conditions over the course of the following summer. May is generally the first month of the year at Harvard Forest in which potential evapotranspiration outflux has the potential to exceed precipitative influx. If the AWC is anomalously low at the end of May, the following summer will have double the chance of ending in an AWC deficit, defined as the case where potential evaporation drains the AWC (Figure 10). Additionally, the AWC deficits of summers that followed dry springs were of greater magnitude than the deficit summers that had wetter springs. The reverse is true of summers that ended in AWC surplus–surplus summers with wetter springs had a greater magnitude of surplus than surplus summers with drier springs. Thus, positive moisture feedback loops at Harvard Forest have the potential to enhance and prolong extreme events.

5. Conclusions

Although drier soils are assumed to be an effect of drier weather, they also play a critical role in causing drier weather in the Northeastern U.S. In this study, we explored the mechanisms driving the paradoxical gap between increasing Northeastern U.S. precipitation influx and concurrent soil water depletion by linking soil water holding capacity with convectively favorable atmospheric conditions. We found that land-atmosphere coupling at Harvard Forest is principally controlled by the timing of precipitation in relation to the available water holding capacity of the soil. As the climate warms and the atmosphere increases its water holding capacity, the increasingly infrequent, high intensity precipitation events in the Northeastern U.S. will result in a greater percentage of water becoming unavailable to evapotranspiration within upland ecosystems due to deep percolation

loss and runoff. As a result, drier soils have a higher associated LCL and contribute a smaller percentage of moisture to the atmospheric water column than wetter soils, which can suppress convective activation. Therefore, drier soils are less capable of maintaining the necessary conditions for rain which strengthens a positive soil moisture feedback loop. Soil texture plays a crucial role in modulating ecosystem water availability, reinforcing the idea that while vegetation–atmosphere exchanges are driven by atmospheric conditions and mediated by plant adjustments, their ultimate outcomes are largely determined by the soil (Wankmüller et al., 2024). This study also indicated that land-atmosphere coupling dynamics, previously thought to be marginal in the Northeastern U.S., may in fact be a critical factor in governing local weather patterns and shaping summer climates into the future. Water availability in mesic temperate forests is closely linked to the carbon cycle, and changes to water availability could play a critical role in limiting carbon uptake within this region with climate change (Feldman et al., 2024; Zhang et al., 2020). It is vital to continue collecting data and producing mechanistic insights into how landscapes directly impact atmospheric conditions, especially as water management grows increasingly challenging for Northeastern U.S. communities as increases in precipitation and more frequent summer dry periods grow beyond historical experience.

Conflict of Interest

The authors declare no conflicts of interest relevant to this study.

Data Availability Statement

Climate data from Harvard Forest weather stations used for long term precipitation trends were accessed through the facilities at Harvard Forest (Boose, 2024; Boose & Gould, 2024). Hydrological station data used to quantify runoff were retrieved from the Harvard Forest hydrological database (Boose & VanScoy, 2024). Soil water datasets were obtained from the Harvard Forest soil moisture network (Frey & Melillo, 2024). Data from the Harvard Forest Hemlock and EMS flux towers were accessed through the Harvard Forest flux network (Matthes et al., 2024; Munger & Hadley, 2024; Munger & Wofsy, 2024). NEON datasets, including eddy covariance products (NEON, 2024a), spectral sun photometer products (NEON, 2024b), soil physical properties (NEON, 2024c), and soil water content (NEON, 2024d), were downloaded from the NEON data portal. Planetary boundary layer height data were retrieved from the NCEP North American Regional Reanalysis (NARR) website (Mesinger et al., 2006). Code for calculating the LCL height (version 1.1) was accessed from the author's website https://romps.berkeley.edu/papers/pubs-2016-lcl.html (Romps, 2017b). The R package ClimClass (Version 2.1.0), was used for calculating Thornthwaite water balances, and was sourced from https://cran.r-project.org/web/packages/ClimClass/index.html (Eccel et al., 2016). The R scripts used to generate the figures and execute the analyses in the paper are licensed under MIT and can be found on GitHub (Jurado, 2024).

Acknowledgments
We would like to extend our sincere gratitude to Dr. Arthur DeGaetano for his valuable advice and expert input throughout this research. We are grateful for the long-term work of Steven Wofsy and J. William Munger in stewarding the data collection at the Harvard Forest EMS tower and making the data openly available. We also wish to acknowledge AERONET for their significant efforts in establishing and maintaining the HARV site spectrophotometer, particularly the contributions of Janae Csavina. Our appreciation goes to the NOAA PSL for providing the NCEP North American Regional Reanalysis (NARR) dataset. The National Ecological Observatory Network (NEON) is a program sponsored by the National Science Foundation and operated under cooperative agreement by Battelle. This material is based in part upon work supported by the National Science Foundation through the NEON Program. We also gratefully acknowledge the support from the Department of Energy Earth & Environmental Systems Grant DE-SC0024092, the Department of Energy Ameriflux Management Program, the National Science Foundation (NSF) LTER program grant DEB-1832210, the NSF Research Experience for Undergraduates program grant DBI-1950364, and NSF grant DEB-1945921.

References

Agel, L., Barlow, M., Qian, J.-H., Colby, F., Douglas, E., & Eichler, T. (2015). Climatology of daily precipitation and extreme precipitation events in the Northeast United States. *Journal of Hydrometeorology*, *16*(6), 2537–2557. https://doi.org/10.1175/jhm-d-14-0147.1

Alessi, M. J., Herrera, D. A., Evans, C. P., DeGaetano, A. T., & Ault, T. R. (2022). Soil moisture conditions determine land-atmosphere coupling and drought risk in the northeastern United States. *Journal of Geophysical Research: Atmospheres*, *127*(6). https://doi.org/10.1029/2021jd034740

Boose, E. (2024). Fisher meteorological station at Harvard forest since 2001. Harvard forest data Archive: HF001 (v.31) [dataset]. Environmental Data Initiative. https://doi.org/10.6073/pasta/bf7a003e4d5352d1e9069422406b6d99

Boose, E., & Gould, E. (2024). Harvard forest climate data since 1964. Harvard forest data Archive: HF300 (v.9) [dataset]. *Environmental Data Initiative*. https://doi.org/10.6073/pasta/a7eb36231cbed30cea58b77af62945f1

Boose, E., & VanScoy, M. (2024). *Prospect Hill hydrological stations at Harvard forest since 2005. Harvard forest data archive: HF070 (v.36)*. Environmental Data Initiative. https://doi.org/10.6073/pasta/5811c1e815ca6a07859b99fbe6d07a30

Ciolkosz, E. J., Waltman, W. J., Simpson, T. W., & Dobos, R. R. (1989). Distribution and genesis of soils of the Northeastern United States. *Geomorphology*, *2*(1–3), 285–302. https://doi.org/10.1016/0169-555x(89)90016-0

Douville, H., Raghavan, K., Renwick, J., Allan, R. P., Arias, P. A., Barlow, M., et al. (2021). In *Water cycle changes. Pages 1055–1210 in V. Masson-Delmotte, et al., eds. Climate Change 2021: The Physical Science Basis*. Cambridge University Press.

Eccel, E., Cordano, E., & Toller, G. (2016). ClimClass: Climate classification according to several indices. *R package version 2.1.0, [Software]*. https://CRAN.R-project.org/package=ClimClass

Feldman, A. L., Feng, X., Felton, A. J., Konings, A. G., Knapp, A. K., Biederman, J. A., & Poulter, B. (2024). Plant responses to changing rainfall frequency and intensity. *Nature Reviews Earth & Environment*, *5*(4), 276–294. https://doi.org/10.1038/s43017-024-00534-0

Findell, K. L., & Eltahir, E. A. (2003). Atmospheric controls on soil moisture–boundary layer interactions. part II: Feedbacks within the Continental United States. *Journal of Hydrometeorology*, *4*(3), 570–583. https://doi.org/10.1175/1525-7541(2003)004<0570:acosml>2.0.co;2

Finzi, A. C., Giasson, M.-A., Barker Plotkin, A. A., Aber, J. D., Boose, E. R., Davidson, E. A., et al. (1960). Relationship of texture classes of fine earth to readily available water. *7th International Congress of Soils Science*, *1*, 354–363.

Fischer, E. M., Seneviratne, S. I., Lüthi, D., & Schär, C. (2007). Contribution of land-atmosphere coupling to recent European summer heat waves. *Geophysical Research Letters*, *34*(6). https://doi.org/10.1029/2006gl029068
Foster, D. R., & Aber, J. D. (2004). *Forests in time: The environmental consequences of 1000 years of change in new England*. Yale University Press.
Frey, S. D., & Melillo, J. M. (2024). Prospect Hill soil warming experiment at Harvard forest since 1991(ver 37) [dataset]. *Environmental Data Initiative*. https://doi.org/10.6073/pasta/abf59a218a5868baf5b2c073a7dd1d7f
Gao, X., Gray, J. M., & Reich, B. J. (2021). Long-term, medium spatial resolution annual land surface phenology with a Bayesian hierarchical model. *Remote Sensing of Environment*, *261*, 112484. https://doi.org/10.1016/j.rse.2021.112484
Green, J. K., Konings, A. G., Alemohammad, S. H., Berry, J., Entekhabi, D., Kolassa, J., et al. (2017). Regionally strong feedbacks between the atmosphere and Terrestrial Biosphere. *Nature Geoscience*, *10*(6), 410–414. https://doi.org/10.1038/ngeo2957
Gu, L., Meyers, T., Pallardy, S. G., Hanson, P. J., Yang, B., Heuer, M., et al. (2006). Direct and Indirect effects of atmospheric conditions and soil moisture on surface energy partitioning revealed by a prolonged drought at a temperate forest site. *Journal of Geophysical Research*, *111*(D16). https://doi.org/10.1029/2006JD007161
Hayhoe, K., Wake, C. P., Huntington, T. G., Luo, L., Schwartz, M. D., Sheffield, J., et al. (2007). Past and future changes in climate and hydrological indicators in the US northeast. *Climate Dynamics*, *28*(4), 381–407. https://doi.org/10.1007/s00382-006-0187-8
Hipel, K. W., & McLeod, A. I. (1994). *Time series modelling of water Resources and environmental systems*. Elsevier Science.
Huang, H., Patricola, C. M., Winter, J. M., Osterberg, E. C., & Mankin, J. S. (2021). Rise in Northeast US extreme precipitation caused by Atlantic variability and climate change. *Weather and Climate Extremes*, *33*, 100351. https://doi.org/10.1016/j.wace.2021.100351
Humphrey, V., Berg, A., Ciais, P., Gentine, P., Jung, M., Reichstein, M., et al. (2021). Soil moisture–atmosphere feedback Dominates land carbon uptake variability. *Nature*, *592*(7852), 65–69. https://doi.org/10.1038/s41586-021-03325-5
Jurado. (2024). sam_jurado/NEUS-HARV: Version 1.0.0 [Software]. *Github*. https://doi.org/10.5281/zenodo.14755493
Kern, J. S. (1995). Geographic patterns of soil water-holding capacity in the contiguous United States. *Soil Science Society of America Journal*, *59*(4), 1126–1133. https://doi.org/10.2136/sssaj1995.03615995005900040026x
Koster, R. D., Dirmeyer, P. A., Guo, Z., Bonan, G., Chan, E., Cox, P., et al. (2004). Regions of strong coupling between soil moisture and precipitation. *Science*, *305*(5687), 1138–1140. https://doi.org/10.1126/science.1100217
Koster, R. D., Sud, Y. C., Guo, Z., Dirmeyer, P. A., Bonan, G., Oleson, K. W., et al. (2006). Glace: The global land–atmosphere coupling experiment. Part I: Overview. *Journal of Hydrometeorology*, *7*(4), 590–610. https://doi.org/10.1175/jhm510.1
Lee, X. (2018). *Fundamentals of boundary-layer meteorology* (pp. 223–226). Springer Atmospheric Sciences. https://doi.org/10.1007/978-3-319-60853-2
Luo, Y., Berbery, E. H., Mitchell, K. E., & Betts, A. K. (2007). Relationships between land surface and near-surface atmospheric variables in the NCEP North American regional reanalysis. *Journal of Hydrometeorology*, *8*(6), 1184–1203. https://doi.org/10.1175/2007jhm844.1
Matthes, J. H., Munger, J. W., & Wofsy, S. (2024). Biomass inventories at Harvard forest EMS tower since 1993 ver 41[dataset]. *Environmental Data Initiative*. https://doi.org/10.6073/pasta/71a1eda9abc2cd1f7cfef62a30460136
Mesinger, F., Dimego, G., Kalnay, E., Mitchell, K., Shafran, P. C., Ebisuzaki, W., et al. (2006). A long-term, consistent, high-resolution climate dataset for the North American domain, as a major improvement upon the earlier global reanalysis datasets in both resolution and accuracy, is presented. [Dataset]. *Bulletin of American Meteorological Society*. Retrieved from https://psl.noaa.gov/data/gridded/data.narr.html
Munger, J. W., & Hadley, J. (2024). Microclimate at Harvard forest HEM, LPH and EMS towers since 2005 ver 28[dataset]. *Environmental Data Initiative*. https://doi.org/10.6073/pasta/6835bb01e61dd0b54af75677104344c3
Munger, J. W., Nadelhoffer, K. J., Ollinger, S. V., Orwig, D. A., Pederson, N., Richardson, A. D., et al. (2020). Carbon budget of the Harvard forest long-term ecological research site: Pattern, process, and response to global change. *Ecological Monographs*, *90*(4), e01423. https://doi.org/10.1002/ecm.1423
Munger, W., & Wofsy, S. (2024). Canopy-atmosphere exchange of carbon, water and energy at Harvard forest EMS tower since 1991. *Harvard Forest Data Archive: HF004 (v.36) [Dataset]. Environmental Data Initiative*. https://doi.org/10.6073/pasta/56c6fe02a07e8a8aaff44a43a9d9a6a5
NEON (National Ecological Observatory Network). (2024a). Bundled data products - Eddy covariance (DP4.00200.001). *RELEASE-2024 [Dataset]*. https://doi.org/10.48443/j9pt-m241
NEON (National Ecological Observatory Network). (2024c). Soil physical and chemical properties, Megapit (DP1.00096.001) [Dataset]. *RELEASE-2024*. https://doi.org/10.48443/s6nd-q840
NEON (National Ecological Observatory Network). (2024d). Soil water content and water salinity (DP1.00094.001), [Dataset]. *RELEASE-2024*. https://doi.org/10.48443/a8vy-y813
NEON (National Ecological Observatory Network). (2024b). Spectral sun photometer - Calibrated sky radiances (DP1.00043.001), provisional data. *Dataset*. Retrieved from https://data.neonscience.org/data-products/DP1.00043.001
Olafsdottir, H. K., Rootzén, H., & Bolin, D. (2021). Extreme rainfall events in the Northeastern USA become more frequent with rising temperatures, but their intensity distribution remains stable. *Journal of Climate*, 1–51. https://doi.org/10.1175/jcli-d-20-0938.1
Pastorello, G., Trotta, C., Canfora, E., Chu, H., Christianson, D., Cheah, Y.-W., et al. (2020). The FLUXNET2015 dataset and the ONEFlux processing pipeline for eddy covariance data. *Scientific Data*, *7*(1). Article 1. https://doi.org/10.1038/s41597-020-0534-3
Qing, Y., Wang, S., Yang, Z.-L., Gentine, P., Zhang, B., & Alexander, J. (2023). Accelerated soil drying linked to increasing evaporative demand in wet regions. *Npj Climate and Atmospheric Science*, *6*(1). Article 1. https://doi.org/10.1038/s41612-023-00531-y
Richardson, A. D., Denny, E. G., Siccama, T. G., & Lee, X. (2003). Evidence for a rising cloud ceiling in eastern north America. *Journal of Climate*, *16*(12), 2093–2098. https://doi.org/10.1175/1520-0442(2003)016<2093:efarcc>2.0.co;2
Robertson, B. B., Almond, P. C., Carrick, S. T., Penny, V., Eger, A., Chau, H. W., & Smith, C. M. S. (2021). The influence of rock fragments on field capacity water content in stony soils from hard sandstone alluvium. *Geoderma*, *389*, 114912. https://doi.org/10.1016/j.geoderma.2020.114912
Romps, D. M. (2017). Exact expression for the lifting condensation level. *Journal of the Atmospheric Sciences*, *74*(12), 3891–3900. https://doi.org/10.1175/jas-d-17-0102.1
Romps, D. M. (2017b). Exact expression for the lifting condensation level (Version 1.1) [Software]. *Author's website*. https://romps.berkeley.edu/papers/pubs-2016-lcl.html
Sen, P. K. (1968). Estimates of the regression coefficient based on Kendall's tau. *Journal of the American Statistical Association*, *63*, 1379–1389. https://doi.org/10.1080/01621459.1968.10480934
Siqueira, M., Katul, G., & Porporato, A. (2009). Soil moisture feedbacks on convection triggers: The role of soil–plant hydrodynamics. *Journal of Hydrometeorology*, *10*(1), 96–112. https://doi.org/10.1175/2008jhm1027.1
Thornthwaite, C. W., & Mather, J. R. (1955). *The water balance* (Vol. 8, pp. 5–86). Publications in climatology.

Urbanski, S., Barford, C., Wofsy, S., Kucharik, C., Pyle, E., Budney, J., et al. (2007). Factors controlling CO2 exchange on timescales from hourly to decadal at Harvard Forest. *Journal of Geophysical Research*, *112*(G2). https://doi.org/10.1029/2006JG000293

Wankmüller, F. J. P., Delval, L., Lehmann, P., Baur, M. J., Cecere, A., Wolf, S., et al. (2024). Global influence of soil texture on ecosystem water limitation. *Nature*, *635*, 631–638. https://doi.org/10.1038/s41586-024-08089-2

Wofsy, S. C., Goulden, M. L., Munger, J. W., Fan, S.-M., Bakwin, P. S., Daube, B. C., et al. (1993). Net exchange of CO2 in a Mid-Latitude forest. *Science*, *260*(5112), 1314–1317. https://doi.org/10.1126/science.260.5112.1314

Zhang, Y., Parazoo, N. C., Williams, A. P., Zhou, S., & Gentine, P. (2020). Large and projected strengthening moisture limitation on end-of-season photosynthesis. *Proceedings of the National Academy of Sciences*, *117*(17), 9216–9222. https://doi.org/10.1073/pnas.1914436117

Zhou, S., Williams, A. P., Berg, A. M., Cook, B. I., Zhang, Y., Hagemann, S., et al. (2019). Land–atmosphere feedbacks exacerbate concurrent soil drought and atmospheric aridity. *Proceedings of the National Academy of Sciences*, *116*(38), 18848–18853. https://doi.org/10.1073/pnas.1904955116